Supramolecular Chemistry

Metal–Organic Rotaxane Frameworks: Three-Dimensional Polyrotaxanes from Lanthanide-Ion Nodes, Pyridinium *N*-Oxide Axles, and Crown-Ether Wheels**

*Dennis J. Hoffart and Stephen J. Loeb**

The dynamic nature of mechanically interlocked molecules has been shown to be particularly useful for the construction of molecular machines.[1] A great deal of information about the potential for the fabrication of nanoscale devices from these units has been gleaned from studies of their fundamental properties in solution.[2] The incorporation of these individual molecular components into the repeating framework of crystalline materials provides a simple method for imposing the type of higher order required for future applications.[3]

A simple interlocked unit from which various types of molecular machines have been constructed is the [2]rotaxane. We have recently shown that a [2]pseudorotaxane comprising a dipyridinium axle and a dibenzo-[24]crown-8 ether (DB24C8) wheel[4] could be used to construct solid-state materials in the form of coordination polyrotaxanes in which every bridging ligand is a [2]rotaxane.[5] These materials contained varying degrees of porosity as there was no detectable interpenetration of nets[6] even though the metal–metal distances are over 22 Å.[7] Unfortunately, regardless of the metal to ligand ratio, a two-dimensional (2D) square net was the highest order attainable with this dynamic ligand and d block transition-metal ions. It was rationalized that a three-dimensional (3D) network was simply not possible owing to the crowding occurring on placing six of these sterically demanding ligands around a single metal ion. To circumvent this problem the dipyridinium ligand was extended by forming the bis(*N*-oxide) analogue, axle $\mathbf{1}^{2+}$. This new axle was prepared from the reaction of 4,4′-bipyridine mono-*N*-oxide with 1,2-dibromoethane and subsequent anion exchange to triflate utilizing the same conditions used to make the bis(4,4′bipyridinium)ethane axle.[4b,8] Scheme 1 shows the conversion of the new bis(*N*-oxide) axle $\mathbf{1}^{2+}$ into a [2]pseudorotaxane, $\mathbf{2}^{2+}$ employing DB24C8 as the wheel. In MeCN, $\mathbf{1}^{2+}$ has an association constant, K_a, of 1125 M^{-1} with DB24C8 as measured by ^{1}H NMR spectroscopy.[9]

[*] D. J. Hoffart, Prof. S. J. Loeb
Department of Chemistry and Biochemistry
University of Windsor
Windsor, ON N9B 3P4 (Canada)
Fax: (+1) 519-973-7098
E-mail: loeb@uwindsor.ca

[**] We thank NSERC of Canada for financial support of this research. DJH thanks the University of Windsor's Centre for Catalysis and Materials Research and ORDCF for the award of a graduate scholarship. Dr. Jorge Tiburcio is thanked for his help with powder XRD measurements.

Supporting information for this article is available on the WWW under http://www.angewandte.org or from the author.

 DOI: 10.1002/ange.200461707

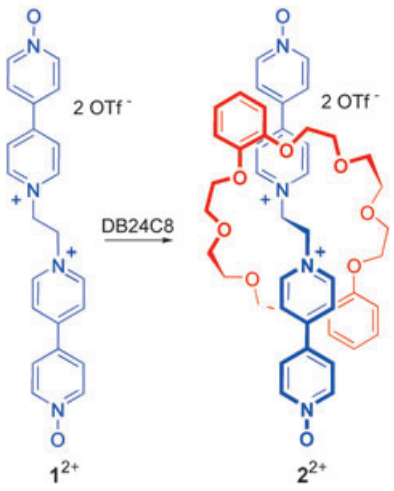

Scheme 1. The formation of a [2]pseudorotaxane ligand from a pyridinium *N*-oxide axle and a dibenzo-[24]crown ether wheel.

The only 3D metal containing polyrotaxane reported to date is that of Kim and co-workers.[10] Under hydrothermal conditions, cyano functional groups on a [2]pseudorotaxane, constructed from a diaminoalkane axle and a cucurbituril wheel, were converted into carboxylate groups in the presence of $Tb(NO_3)_3$. Herein, we report that the *N*-oxide version of our [2]pseudorotaxane motif,[4] $\mathbf{2}^{2+}$, can be employed in simple room-temperature, metal–ligand self-assembly (crystal engineering) reactions using lanthanide ions[11] to form two distinctly different types of 3D, metal–organic framework materials containing [2]rotaxanes.

Three equivalents of $\mathbf{1}[OTf]_2$ (OTf = triflate, $[CF_3SO_3]^-$) were mixed with nine equivalents of DB24C8 and one equivalent of $[M(OTf)_3]$ (M = Sm, Eu, Gd, Tb) in MeCN. X-ray quality crystalline material[12] was produced in moderate yield (≈50% on average). Figure 1 shows that the use of Ln^{III} ions as nodes results in an eight-coordinate metal center with a square antiprismatic geometry comprising six [2]rotaxane ligands, one water molecule, and one coordinated $[OTf]^-$ ion.

Figure 2 shows how propagation of the eight-coordinate units results in 3D, metal–organic frameworks $[M(H_2O)(OTf)(\mathbf{2})_3][Cl][OTf]_7$ (M = Sm (**3**), Eu (**4**), Gd (**5**), Tb (**6**); for the source of the Cl ion see ref. [12]) in which every bridging ligand is a [2]rotaxane. The "square" sides of the α-polonium type net are defined by Sm···Sm separation of approximately 23.5 Å. The cavity has a volume of about 10000 $Å^3$, however this space is filled by the interpenetration of a parallel net. (See Supporting Information for diagrams depicting single interpenetration of the two lattices). The longer *N*-oxide axle results in an elongation of the metal–metal separation which creates an expanded cavity which can now accommodate the girth of the [2]rotaxane ligand. Of note is that only a single interpenetration occurs within such a large volume.

Although an isomorphous series (Sm, Eu, Gd, Tb) of 3D polyrotaxanes could be produced with eight-coordinate metal centers, we found that changing to a metal ion with a slightly smaller radius, Yb^{III} (2.40 Å versus 2.51 Å for Tb, 2.59 Å for Sm), yielded another 3D polyrotaxane but with a distinctly different solid-state structure. Large crystals of $[Yb(OTf)(\mathbf{2})_3][Cl][OTf]_7$ (**7**) were isolated in moderate yield from the slow

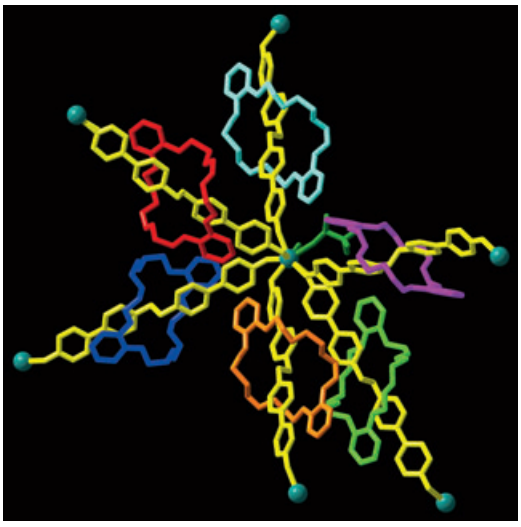

Figure 1. A ball-and-stick representation of the metal–ligand coordination sphere around Sm^{III} in $\mathbf{3}^{8+}$; solvent, noncoordinating anions and hydrogen atoms have been removed for clarity. Key: $\mathbf{1}^{2+}$ axle is shown in yellow; DB24C8 wheels are shown in red, blue, orange, light green, purple, cyan; coordinated water and triflate anion are shown in dark green; Sm metal ions are shown in gray.

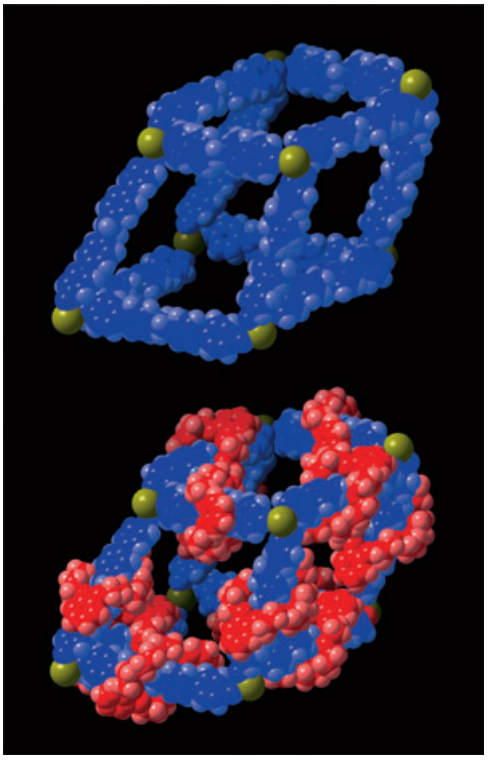

Figure 2. Top: A space-filling model showing a single "cube" unit of the 3D network for $\mathbf{3}^{8+}$ with the molecules of DB24C8 removed for clarity. Bottom: The same framework with the DB24C8 units included. Key: The 3D metal–ligand framework is shown in blue; the molecules of DB24C8 are shown in red; the Sm metal ions in gold.

diffusion of a solution of $Yb(OTf)_3$ into a solution of the [2]pseudorotaxane ligand $\mathbf{2}(OTf)_2$ at room temperature. The Yb^{III} center adopts a seven-coordinate pentagonal bipyramidal geometry, with five *N*-oxide rotaxanes occupying the equatorial sites of the pentagonal plane and one further [2]rotaxane and a single triflate ion positioned in the axial sites. The metal core and ligand set for $\mathbf{7}^{8+}$ are shown in Figure 3.

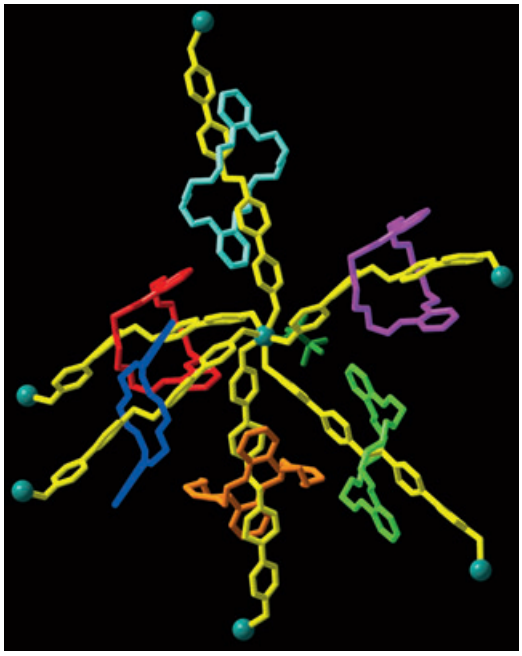

Figure 3. A ball-and-stick representation of the metal–ligand coordination sphere around Yb^{III} in $\mathbf{7}^{8+}$; solvent, noncoordinating anions, and hydrogen atoms have been removed for clarity. Key: $\mathbf{1}^{2+}$ axle is shown in yellow; DB24C8 wheels are shown in red, blue, orange, light green, purple, cyan; coordinated triflate anion is shown in green; Yb metal ions shown in gray.

The planar tessellation of a five-coordinate node into a 2D network is formally impossible, but this is what in fact occurs. Each *N*-oxide ligand can "bend" at the Yb-O-N linkage and this results in a [3/4,5] net comprising alternating triangles and squares linked through five-connected nodes.[13] Until very recently,[14] this 2D pattern was unknown in chemical systems. Figure 4 shows the tiling in the pentagonal plane. This network propagates one step further into a full 3D metal–organic framework by pillaring to adjoining layers through the sixth [2]rotaxane in the apical position. This results in a previously unknown topology and takes the form of a [3/4/6,6] 6-connected net comprised of triangles, squares, and hexagons. The square cavities are used for interpenetration of these nets in a manner conceptually similar to those of **3**–**6**. Interpenetration is not possible through the more crowded triangular cavities. (See Supporting Information for diagrams depicting the full 3D structure and associated interpenetration of the lattices).

Both sorts of materials (**3**–**6** and **7**) show similar stability as determined by thermogravimetric analysis (TGA) and powder X-ray diffraction (PXRD) measurements.[15] Solvents

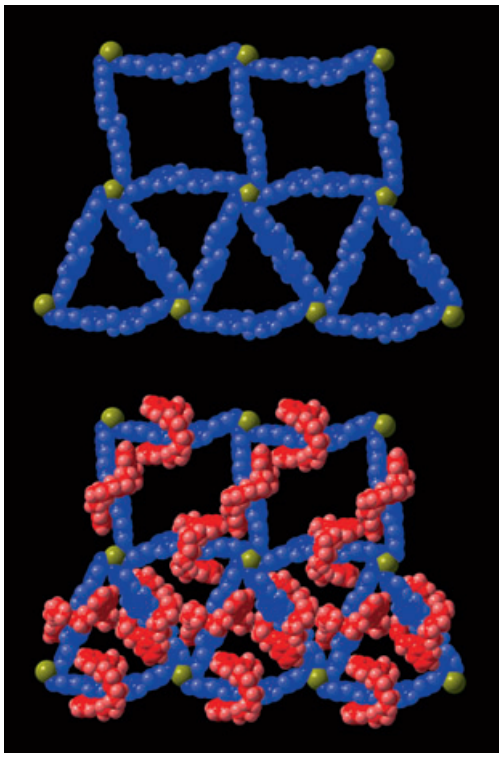

Figure 4. Top: A space-filling model of $\mathbf{7}^{8+}$ showing the 2D pentagonal network [3/4,5] plane with the molecules of DB24C8 removed for clarity. The apical [2]rotaxane has also been removed for clarity. Bottom: The same framework with the DB24C8 molecules shown. Key: The 3D metal–ligand framework is shown in blue; the molecules of DB24C8 are shown in red; the Yb metal ions in gold.

of crystallization (MeCN, H_2O) were easily lost at temperatures ranging from 25–80 °C followed by phase stability until approximately 240 °C. PXRD patterns of the desolvated materials were consistent with retention of the 3D framework. Release of the trapped crown ether was only observed at >240 °C, which also indicates that the 3D metal ligand framework is intact until this temperature. Thus, although the [2]rotaxanes are initially formed with weak noncovalent interactions, a strong metal–ligand bond must be broken to release the interlocked macrocycle from the metal–organic skeleton.

From these results, we can conclude that 1) the design of soft materials with interlocked components (metal–organic rotaxane frameworks: MORFs) can be expanded to include pyridinium *N*-oxide axles and crown-ether wheels, 2) it is possible to create fully 3D structures in which every linker is a pyridinium-based rotaxane, and 3) interpenetration of these rotaxane nets is a possibility since the openings created are large enough for these uncommonly "wide" ligands to fit through the pores.

Received: August 18, 2004
Revised: October 28, 2004
Published online: December 28, 2004

Keywords: coordination polymers · crown compounds · lanthanides · rotaxanes · self-assembly

[1] a) J. F. Stoddart, *Acc. Chem. Res.* **2001**, *34*, 410; b) A. R. Pease, J. O. Jeppesen, J. F. Stoddart, Y. Luo, C. P. Collier, J. R. Heath, *Acc. Chem. Res.* **2001**, *34*, 433; c) J.-P. Collin, C. Dietrich-Buchecker, P. Gaviña, M. C. Jiminez-Molero, J.-P. Sauvage, *Acc. Chem. Res.* **2001**, *34*, 477; d) A. N. Shipway, I. Willner, *Acc. Chem. Res.* **2001**, *34*, 421.

[2] a) V. Balzani, A. Credi, F. M. Raymo, J. F. Stoddart, *Angew. Chem.* **2000**, *112*, 3484; *Angew. Chem. Int. Ed.* **2000**, *39*, 3348; b) R. Ballardini, V. Balzani, A. Credi, M. T. Gandolfi, M. Venturi, *Acc. Chem. Res.* **2001**, *34*, 445.

[3] a) M. Albrecht, M. Lutz, A. L. Spek, G. van Koten, *Nature* **2000**, *406*, 970; b) O. M. Yaghi, M. O'Keefe, N. W. Ockwing, H. K. Chae, M. Eddaoudi, J. Kim, *Nature* **2003**, *423*, 705.

[4] a) S. J. Loeb, J. A. Wisner, *Angew. Chem.* **1998**, *110*, 3010; *Angew. Chem. Int. Ed. Engl.* **1998**, *37*, 2838; b) S. J. Loeb, J. A. Wisner, *Chem. Commun.* **1998**, 2757.

[5] G. J. E. Davidson, S. J. Loeb, *Angew. Chem.* **2003**, *115*, 78; *Angew. Chem. Int. Ed.* **2003**, *42*, 74.

[6] M. Zaworotko, *Chem. Commun.* **2001**, 1.

[7] N. G. Pschirer, D. M. Ciurtin, M. D. Smith, U. H. F. Bunz, H-C. zur Loye, *Angew. Chem.* **2002**, *114*, 663; *Angew. Chem. Int. Ed.* **2002**, *41*, 583.

[8] M. I. Attalla, N. S. McAlpine, L. A. Summers, *Z. Naturforsch. B* **1984**, *39*, 74.

[9] This value compares well to that of the precursor bis(pyridine) axle which, in MeCN, has $K_a \approx 900\,\mathrm{M}^{-1}$ with DB24C8.

[10] a) E. Lee, J. Heo, K. Kim, *Angew. Chem.* **2000**, *112*, 2811; *Angew. Chem. Int. Ed.* **2000**, *39*, 2699; b) K. M. Park, D. Whang, E. Lee, J. Heo, K. Kim, *Chem. Eur. J.* **2002**, *8*, 498.

[11] For examples of crystal engineering with Ln^{III} ions and pyridine-*N*-oxides see: D. Long, A. J. Blake, N. R. Champness, C. Wilson, M. Schröder, *Chem. Eur. J.* **2002**, *8*, 2026.

[12] Crystal data[16] for **3**: $C_{152}H_{163.75}Cl_{0.5}F_{25.5}N_{14.75}O_{64}S_{8.5}Sm$, $M_r = 4147.7$, orange prisms, ($0.36 \times 0.34 \times 0.26$ mm) triclinic, $P\bar{1}$, $a = 17.5661(13)$, $b = 23.4327(13)$, $c = 27.0910(17)$ Å, $\alpha = 78.0860(10)$, $\beta = 80.5090(10)$, $\gamma = 74.0460(10)°$, $V = 10421.2(12)$ Å^3, $Z = 2$, $\rho_{calcd} = 1.322\,\mathrm{g\,cm^{-3}}$, $\mu = 0.476\,\mathrm{mm^{-1}}$, min/max trans. = 0.8888, $2\theta_{max} = 45.0°$, $Mo_{K\alpha}\lambda = 0.71073$ Å, $T = 100.0(2)$ K, 66987 total reflections (R(int) = 0.0483), $R1 = 0.1248$, $wR2 = 0.3293$ [$I > 2\sigma I$], $R1 = 0.1421$, $wR2 = 0.3522$ [all data], GoF (F^2) = 1.579, $N_o/N_v/N_r = 27216/3064/376$. Data for analogous compounds **4** (Eu), **5** (Gd), and **6** (Tb) were not of sufficient quality to render a full structure solution but unit cells and partial solutions verified that these are isomorphous with **3.** **7**: $C_{160}H_{175.5}ClF_{24}N_{19}O_{59.5}S_8Yb$, $M_r = 4237.7$, yellow prisms, $0.24 \times 0.20 \times 0.18$ mm) triclinic, $P\bar{1}$, $a = 20.495(3)$, $b = 22.701(3)$, $c = 27.435(3)$ Å, $\alpha = 84.146(3)$, $\beta = 78.935(3)$, $\gamma = 67.636(3)°$, $V = 11579(3)$ Å^3, $Z = 2$, $\rho_{calcd} = 1.215\,\mathrm{g\,cm^{-3}}$, $\mu = 0.579\,\mathrm{mm^{-1}}$, min/max trans. = 0.7412, $2\theta_{max} = 50.0°$, $Mo_{K\alpha}\lambda = 0.71073$ Å, $T = 100.0(2)$ K, 40594 total reflections (R(int) = 0.0980), $R1 = 0.1417$, $wR2 = 0.3729$ [$I > 2\sigma I$], $R1 = 0.1841$, $wR2 = 0.4003$ [all data], GoF (F^2) = 1.438, $N_o/N_v/N_r = 40594/2444/294$. The presence of chloride ion in these structures is attributed to small amounts of this anion in the bulk sample of axle $\mathbf{1}^{2+}$ since during work up $\mathbf{1}^{2+}$ is subjected to column chromatography in which one of the solvents is aqueous NH_4Cl before anion exchange to OTf. Crystals of **3**–**7** were frozen in paratone oil inside a cryoloop. Reflection data were integrated from frame data obtained from hemisphere scans on a Brüker APEX diffractometer with CCD detector. Decay was monitored by 50 standard data frames measured at the beginning and end of data collection. Diffraction data and unit-cell parameters were consistent with assigned space groups. Lorentzian polarization corrections and empirical absorption corrections, based on redundant data at varying effective azimuthal angles, were applied to the data sets. The structures were solved by direct methods, completed by subsequent Fourier syntheses and refined with conjugate-gradient least-squares methods against $|F^2|$ data. For both compounds a chloride anion was located and refined instead of one of the triflate anions. All non-hydrogen atoms were refined anisotropically. Hydrogen atoms were treated as idealized contributions. Scattering factors and anomalous dispersion coefficients are contained in the SHELXTL 5.03 program library (G. M. Sheldrick, Madison, WI). CCDC-247756 and CCDC-247757 (**3** and **7**) contain the supplementary crystallographic data for this paper. These data can be obtained free of charge from The Cambridge Crystallographic Data Centre via www.ccdc.cam.ac.uk/data_request/cif.

[13] A. F. Wells, *Three-Dimensional Nets and Polyhedra*, Wiley, New York, **1977**.

[14] a) J.-R. Li, X.-H. Bu, R.-H. Zhang, *Inorg. Chem.* **2004**, *43*, 237; b) X.-H. Bu, W. Weng, W. Chen, R.-H. Zhang, *Inorg. Chem.* **2002**, *41*, 413.

[15] TGA were performed on a Mettler Toledo TGA/SDTA85 Instrument under He(g) atmosphere at scan rate of 5°C/min. PXRD measurements were recorded on a Brüker D8 Discover diffractometer with an AXS HI-STAR area detector using $Cu_{K\alpha}$ radiation.

[16] Ball-and-stick and space-filling diagrams were prepared using DIAMOND-Visual Crystal Structure Information System CRYSTAL IMPACT, Postfach 1251, 53002 Bonn.

